Asymmetry of l^{N+1}-$l^N l'$ transition-array patterns in ionic spectra

C. Bauche-Arnoult and J. Bauche
Laboratoire Aimé Cotton, Centre National de la Recherche Scientifique, Bâtiment 505, 91405 Orsay Cedex, France

M. Klapisch
Racah Institute of Physics, The Hebrew University, 91904 Jerusalem, Israel
(Received 16 July 1984)

Closed-form expressions for the first two moments of the *wave-number distribution* of unresolved transition arrays (UTA's) observed in highly ionized atoms have been published previously. However, this is not sufficient in many observed cases of asymmetrical UTA's. This paper describes a method for the evaluation of the third moment for arrays of frequently observed type l^{N+1}-$l^N l'$. Distributions are represented by skewed Gaussians. The maximum is thus shifted with respect to the average wave number, and the full width at half maximum is smaller than that of a symmetrical Gaussian. Applications to Pr XVI and Xe XXVIII—XXX are presented.

I. INTRODUCTION

It frequently happens, in the emission spectra of highly ionized atoms, that the lines corresponding to the transitions between the levels of two configurations are not separated. This is due to experimental reasons and/or to broadening phenomena in the emitting plasma itself. The corresponding broad peak in the spectrum can be called an unresolved transition array[1-3] (UTA).

It has been proposed recently to characterize such an UTA through the first two moments of the *wave-number distribution,* i.e., its average and its variance. Formulas have been established[1,2] for these quantities in terms of energy radial parameters easily computed *ab initio.* Now, we have observed that in some cases such a two-moment description is too crude because it leaves no other possibility than assuming a symmetrical shape for the array representation (in practice, a Gaussian shape). This symmetrical shape is not adequate, for example, when most weak lines appear in the spectrum on the same side of the intense lines. This is the case of the $4d^8$-$4d^7 4f$ array in the Pr XVI ion, shown in Fig. 1. In this figure the lines of the array are represented by vertical segments. For each of the lines, the length of the segment is proportional to the emission strength, except that the segments which would measure less than 3% of the longest are all conventionally

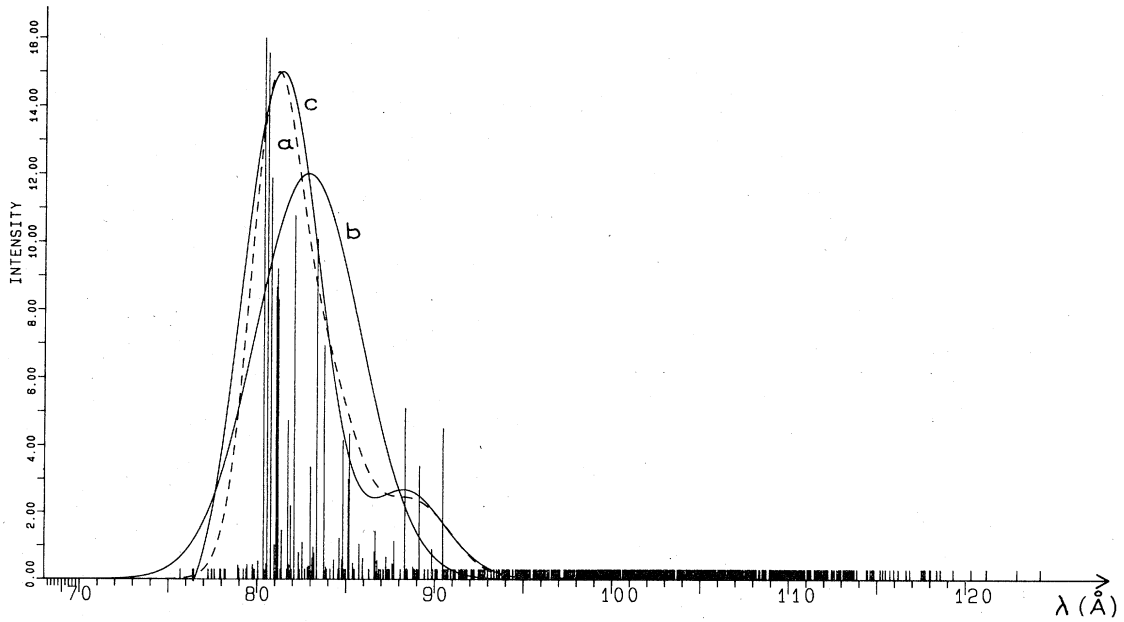

FIG. 1. Pr XVI $4d^8$-$4d^7 4f$ transition array. Each line is represented with a height proportional to its strength, except those with a strength less than 3% of the highest, which have all, conventionally, been represented with this value. (a), envelope calculated by adding the different lines with a given small FWHM (0.5 Å). (b), Gaussian curve, using μ_1 and μ_2^c. (c), skewed Gaussian curve, using μ_1, μ_2^c, and μ_3^c.

lengthened to that 3% limit. It is clear that the pattern is strongly skewed (the curves drawn on Fig. 1 are explained in Sec. IV).

The skewness properties of configurations and transition arrays have already been considered by Moszkowski and Cowan. Moszkowski[4] computed the skewness of a transition array in a very simple case. Cowan[5] calculated explicitly the skewness of the distribution of levels in many configurations (Ref. 5, Table 21-1) and also of several transition arrays.

The aim of this paper is to obtain a general method for evaluating *ab initio* the asymmetry properties of transition arrays, in highly ionized spectra, where the lowest configurations are well separated. For that purpose, we attempted the formal evaluation of the third moment of the weighted wave-number distribution of the l^{N+1}-$l^N l'$ transition array (the most interesting in highly ionized atoms). In the following we show that this rather formidable task is not worth undertaking (Sec. II). For the sake of simplicity, we propose a numerical method in a hydrogenic approximation, which is suitable for the external subshells of highly ionized atoms. In this way, we obtain the asymmetry properties of the main nd^{N+1}-$nd^N n'p$ and nd^{N+1}-$nd^N n'f$ types of arrays (Sec. III). Once a skewed curve shape is assumed, the axis and full width at half maximum (FWHM) of the array fit better the explicitly calculated spectrum (Sec. IV) and the experiment (Sec. V).

II. EVALUATION OF THE THIRD MOMENT OF THE WAVE-NUMBER DISTRIBUTION IN THE nl^{N+1}-$nl^N n'l'$ ARRAY

A. Principles

As in Ref. 1, denoted I in the following, we use the definition

$$\mu_n=\sum_{a,b}[(b\mid H\mid b)-(a\mid H\mid a)]^n w_{ab}/W \tag{1}$$

for the nth moment of the weighted distribution of the line wave numbers. In this equation, H is the sum of the electrostatic and spin-orbit Hamiltonians, the weight w_{ab} of a transition is the z part of its electric dipole strength [$w_{ab}=\mid(a\mid Z\mid b)\mid^2$], $W=\sum_{a,b}w_{ab}$, and the sums run over all the a and b *states* of the lower and higher configurations $A=l^{N+1}$ and $B=l^N l'$, respectively.

The formulas for $n=1$ and 2 have already been determined[1,2] in terms of the Slater and spin-orbit radial integrals and of their squares and cross products. Those for $n=2$ had already been studied by Moszkowski[4] in the assumption that a radial integral with a given name has the same numerical value in both configurations. This assumption leads to simpler results and is consistent with the current use of the central-field *ab initio* method for highly ionized atoms. We have used it throughout the present work for the evaluation of μ_3.

In the same way as in I, we are first interested in dealing with the intermediate-coupling nature of the a and b states and in finding the formal dependence of μ_3 on N. For that purpose, the second-quantization method, introduced by Judd[6] in the field of atomic spectroscopy, is most adequate.

Considering, as an example, the quantity

$$q=\sum_{a,b}(a\mid Z\mid b)(b\mid H\mid b)(b\mid H\mid b)(b\mid H\mid b)(b\mid Z\mid a) \tag{2}$$

occurring in μ_3 [Eq. (1)], and selecting in the $(b\mid H\mid b)$ matrix elements the part in $F^k(l,l')$, we can deal easily with the intermediate coupling and arrive at

$$q=\sum_{a'}(a'\mid Q\mid a') \tag{3}$$

[see Eq. (9) in I], where Q is a sum over magnetic quantum numbers m_l and m_s of a product of many annihilation and creation operators and of matrix elements of z and $g_{12}=e^2/r_{12}$, and where a' is a state of l^{N+1} in any extreme coupling of convenience.

B. N dependence

Rather than computing directly the matrix element q of the very cumbersome operator Q of Eq. (3), it looks more convenient to find first its dependence on N. For example, in the case of interest, Q contains at most four annihilation and four creation operators of l electrons. Moreover, the second-quantization operator for the calculation of the W denominator in Eq. (1) contains one creation-annihilation pair of electrons. In this way, it is found that the coefficients of the triple products of the $F^k(l,l')$ integrals in μ_3 depend on N through polynomials of degree 3.

There occur altogether four *types* of radial Slater and spin-orbit integrals in the level energies, namely $F^k(l,l)$, $F^k(l,l')$ or $G^k(l,l')$, $\zeta_l,\zeta_{l'}$, irrespective of the configuration in which they are considered. This leads to many *types* of triple products. Actually, we are interested in the *centered* moment

$$\mu_3^c=\mu_3-3\mu_2\mu_1+2(\mu_1)^3=\mu_3-3\mu_2^c\mu_1-(\mu_1)^3 \tag{4}$$

rather than in μ_3 itself, μ_2^c being the centered second-order moment, i.e., the variance. This fact and the other assumptions and properties result in several simplifications.

(i) Each triple product which contains only one spin-orbit integral has a null coefficient in μ_3^c. This can be explained, in the same way as the absence of cross products between Slater and spin-orbit integrals in the variance (Sec. III A in I), by the fact that in this case the operator of type Q [Eq. (3)] has tensorial rank 1 in the spin subspace.

(ii) Cancellations occur for the triple products which contain only integrals $F^k(l,l)$ and/or ζ_l, i.e., those integrals which appear in both configurations. As a consequence, the maximum power of N in the polynomial dependence of such products is lower in the third-order moment of the distribution of transition energies than in that of a state-energy distribution. The same phenomenon is well known in the results for the variance μ_2^c, where the maximum power of N for the $F^k(l,l)F^{k'}(l,l)$ products reduces from 4 for the states (Table II in I) to 2 for the transitions (see the top right of p. 2428 in I).

TABLE I. Highest powers in N of the different triple products in μ_3^c, denoted XY. Products which do not appear in this table, or which appear, but without a value given, have a null contribution.

Y \ X	$F^k(l,l)$	$F^k(l,l')$ or $G^k(l,l')$	ζ_l or $\zeta_{l'}$
$F^{k'}(l,l)F^{k''}(l,l)$	3	5	
$F^{k'}(l,l')F^{k''}(l,l')$ or $F^{k'}(l,l')G^{k''}(l,l')$ or $G^{k'}(l,l')G^{k''}(l,l')$	4	3	
$(\zeta_l)^2$, $\zeta_l\zeta_{l'}$, or $(\zeta_{l'})^2$		1	0

(iii) Some simple factors are evident. First, any triple product containing a Slater integral disappears if $N=0$, i.e., in the case of one-electron configurations. Second, if it contains only Slater integrals, it is zero for $N=4l+1$, a case with only one emission line in Russell-Saunders coupling. Therefore the factor N multiplies the former type of products and $4l-N+1$ multiplies the latter type.

(iv) Symmetry properties with respect to the half subshell can be exploited for the triple products of $F^k(l,l)$ integrals and for the triple products of ζ_l and/or $\zeta_{l'}$ integrals. Indeed, replacing N by $4l-N+1$ changes the signs of the coefficients of the former products and leaves invariant those of the latter.

In conclusion, we give in Table I the maximum powers of N for the polynomial dependences of triple products

TABLE II. Formulas for the AAA (S_1), BCC (S_2–S_5), and CCC (S_6–S_9) types of triple-product contributions to μ_3^c.

$$S_1:\ N(4l-N+1)(4l-2N+1)\times\sum_{k\neq0}\sum_{k'\neq0}\sum_{k''\neq0}\frac{(2l+1)^3}{(4l-1)4l(4l+1)^3}\times\left[-2(2l+1)^2(4l+1)^2\begin{Bmatrix}k&k'&k''\\l&l&l\end{Bmatrix}^2+(2l+1)^2(4l+1)^2\begin{Bmatrix}l&l&k\\l&k'&l\\k''&l&l\end{Bmatrix}+3(2l+1)(4l+1)\begin{Bmatrix}l&l&k\\l&l&k'\end{Bmatrix}-6(2l+1)(4l+1)\frac{\delta(k,k')}{2k+1}+2\right]\times\begin{pmatrix}l&k&l\\0&0&0\end{pmatrix}^2\begin{pmatrix}l&k'&l\\0&0&0\end{pmatrix}^2\begin{pmatrix}l&k''&l\\0&0&0\end{pmatrix}^2F^k(l,l)F^{k'}(l,l)F^{k''}(l,l)\ .$$

$$S_2:\ -\frac{N}{4(4l+1)}l(l+1)(2l+1)(2l'+1)\sum_{k\neq0}\begin{Bmatrix}l&l&k\\l'&l'&1\end{Bmatrix}\left[1+(2l+1)\begin{Bmatrix}l&l&k\\l&l&1\end{Bmatrix}\right]\times\begin{pmatrix}l&k&l\\0&0&0\end{pmatrix}\begin{pmatrix}l'&k&l'\\0&0&0\end{pmatrix}F^k(l,l')(\zeta_l-\zeta_{l'})^2\ .$$

$$S_3:\ -\frac{N}{6(4l+1)}l(l+1)(2l+1)(2l'+1)\begin{pmatrix}l&1&l'\\0&0&0\end{pmatrix}^2G^1(l,l')(\zeta_l)^2\ .$$

$$S_4:\ -\frac{N}{6(4l+1)}(2l+1)l'(l'+1)(2l'+1)\begin{pmatrix}l&1&l'\\0&0&0\end{pmatrix}^2G^1(l,l')(\zeta_{l'})^2\ .$$

$$S_5:\ \frac{N}{6(4l+1)}(2l+1)(2l'+1)[l(l+1)+l'(l'+1)-2]\begin{pmatrix}l&1&l'\\0&0&0\end{pmatrix}^2G^1(l,l')\zeta_l\zeta_{l'}\ .$$

$$S_6:\ \tfrac{1}{4}(\tfrac{3}{2})^{1/2}[l(l+1)]^{3/2}(2l+1)^{1/2}\begin{Bmatrix}1&1&1\\l&l&l\end{Bmatrix}(\zeta_l)^3\ .$$

$$S_7:\ \tfrac{3}{4}(\tfrac{3}{2})^{1/2}l(l+1)(2l+1)[l'(l'+1)(2l'+1)]^{1/2}\begin{Bmatrix}1&1&1\\l&l&l\end{Bmatrix}\begin{Bmatrix}l'&1&l'\\l&1&l\end{Bmatrix}(\zeta_l)^2\zeta_{l'}\ .$$

$$S_8:\ -\tfrac{3}{4}(\tfrac{3}{2})^{1/2}l'(l'+1)(2l'+1)[l(l+1)(2l+1)]^{1/2}\begin{Bmatrix}1&1&1\\l'&l'&l'\end{Bmatrix}\begin{Bmatrix}l'&1&l'\\l&1&l\end{Bmatrix}\zeta_l(\zeta_{l'})^2\ .$$

$$S_9:\ -\tfrac{1}{4}(\tfrac{3}{2})^{1/2}[l'(l'+1)]^{3/2}(2l'+1)^{1/2}\begin{Bmatrix}1&1&1\\l'&l'&l'\end{Bmatrix}(\zeta_{l'})^3\ .$$

TABLE III. Values of μ_3^c (in cm^{-3}) and σ (in cm^{-1}) obtained with Slater integrals in hydrogenic ratios, for $Z^*=1$. $k(N)=\mu_3^c(\text{Sl hyd})/[\sigma(\text{SL hyd})]^3$ can be used to compute approximately the contribution of the Slater integrals to μ_3^c.

	N	1	2	3	4	5	6	7	8
	μ_3^c(Sl hyd)	-1576×10^6	-2018×10^6	-1615×10^6	-693×10^6	-401×10^6	1320×10^6	1740×10^6	1375×10^6
$3d^{N+1}$-$3d^N4p$	σ(Sl hyd)	1012.1	1338.9	1518.2	1600.3	1600.3	1518.2	1338.9	1012.1
	k	−1.520	−0.841	−0.462	−0.169	0.098	0.377	0.725	1.326
	μ_3^c(Sl hyd)	-2587×10^6	-4932×10^6	-6850×10^6	-8174×10^6	-8745×10^6	-8401×10^6	-6966×10^6	-4242×10^6
$3d^{N+1}$-$3d^N4f$	σ(Sl hyd)	1240.1	1640.5	1860.1	1960.7	1960.7	1860.1	1640.5	1240.1
	k	−1.357	−1.117	−1.064	−1.084	−1.160	−1.305	−1.578	−2.224
	μ_3^c(Sl hyd)	-1503×10^5	-1929×10^5	-1619×10^5	-858×10^5	94×10^5	974×10^5	1496×10^5	1314×10^5
$4d^{N+1}$-$4d^N5p$	σ(Sl hyd)	450.0	595.4	675.1	711.6	711.6	675.1	595.4	450.0
	k	−1.649	−0.914	−0.526	−0.238	0.026	0.316	0.709	1.442
	μ_3^c(Sl hyd)	-2787×10^5	-7291×10^5	-1237×10^6	-1700×10^6	-2025×10^6	-2119×10^6	-1886×10^6	-1221×10^6
$4d^{N+1}$-$4d^N4f$	σ(Sl hyd)	755.2	999.1	1132.8	1194.1	1194.1	1132.8	999.1	755.2
	k	−0.647	−0.731	−0.851	−0.998	−1.189	−1.458	−1.891	−2.835

occurring in μ_3^c. The triple products not entered in Table I have null coefficients. For the sake of brevity, in the sequel we denote ζ_l and $\zeta_{l'}$ by C, whereas $F^k(l,l)$ and $F^k(l,l')$ or $G^k(l,l')$ are denoted A and B, respectively.

C. Formal calculations

Formal calculations of Eq. (1) for $n>1$ by Racah's methods[7] lead to formulas without sums involving coefficients of fractional parentage only when $N=0$, 1, $4l$, and $4l+1$. From the information given in Sec. II B above, it can be concluded that, in the present problem, all contributions entered in Table I can be computed in this way except those with a highest power in N larger than 3. We give in Table II the results for the cases AAA, BCC, and CCC. Those for BBB, which are very lengthy, have been computed only in two cases, namely, for the triple products of $F^k(l,l')$ integrals and for those of $G^k(l,l')$ integrals; they are available upon request.

In Table II the following points are noteworthy: the $G^k(l,l')$ integrals with $k\neq1$ do not contribute to S_3-S_5, in S_2 only the difference between the spin-orbit constants occurs; and the sum $S_6+S_7+S_8+S_9$ changes sign upon $l\leftrightarrow l'$ interchange.

III. NUMERICAL CALCULATION: THE HYDROGENIC ASSUMPTION

Because we have not obtained a complete closed formula for μ_3^c, we propose now an alternative procedure for evaluating it, in a hydrogenic approximation. In this assumption we consider that the ion is sufficiently ionized so that the ratios between Slater energy integrals are the same as for hydrogenic radial functions. We recall that for a given nuclear charge Z^*, all Slater integrals are proportional to Z^*, so that their ratios are independent of Z^*. Then, in a given series in N of nl^{N+1}-$nl^N n'l'$ arrays, the total contribution μ_3^c (Sl hyd) of the upper two lines of Table I is the product of $(Z^*)^3$ by a function of N only. Now, because it contains the factor $N(4l-N+1)$ [see Sec. II B, (iii)], this function can be determined completely by means of its explicit numerical calculation (diagonalization of the electrostatic Hamiltonian with hydrogenic integral ratios) for four values of N ($N\neq0,4l+1$).

We have done this for four series of current interest in atomic ions, $3d^{N+1}$-$3d^N4p$, $3d^{N+1}$-$3d^N4f$, $4d^{N+1}$-$4d^N5p$, and $4d^{N+1}$-$4d^N4f$. The results for the quantity μ_3^c (Sl hyd) are listed in Table III, together with $\sigma(\text{Sl hyd})\equiv[\mu_2^c(\text{Sl hyd})]^{1/2}$, for $Z=1$.

Thus, in all cases of practical interest we propose to evaluate μ_3^c as the sum of two parts.

(i) An approximate value of the Slater part μ_3^c(Sl) (the upper two lines of Table I) in which we propose to avoid the necessity of estimating Z^* by the following scaling:

$$\mu_3^c(\text{Sl})=\mu_3^c(\text{Sl hyd})[\sigma(\text{Sl})/\sigma(\text{Sl hyd})]^3 . \tag{5}$$

We rewrite this equation as

$$\mu_3^c(\text{Sl})=k(N)[\sigma(\text{Sl})]^3 , \tag{6}$$

where the value of the dimensionless factor $k(N)$ can be found in Table III for each of the four series of interest,

TABLE IV. Numerical evaluation of S_2–S_9 for usual types of arrays.

	p^{N+1}-$p^N s$	p^{N+1}-$p^N d$	d^{N+1}-$d^N p$	d^{N+1}-$d^N f$	f^{N+1}-$f^N d$
S_2: $NF^2(l,l')(\zeta_l-\zeta_{l'})^2$		0.03	0.016 667	0.019 048	0.013 187
$NF^4(l,l')(\zeta_l-\zeta_{l'})^2$				0.026 455	0.018 315
S_3: $NG^1(l,l')(\zeta_l)^2$	−0.066 667	−0.133 333	−0.222 222	−0.333 333	−0.461 538
S_4: $NG^1(l,l')(\zeta_{l'})^2$		−0.4	−0.074 074	−0.666 667	−0.230 769
S_5: $NG^1(l,l')\zeta_l\zeta_{l'}$		0.4	0.222 222	0.888 889	0.615 385
S_6: $(\zeta_l)^3$	0.25	0.25	0.75	0.75	1.5
S_7: $(\zeta_l)^2\zeta_{l'}$		−1.125	−1.125	−3.0	−3.0
S_8: $(\zeta_l)(\zeta_{l'})^2$		1.125	1.125	3.0	3.0
S_9: $(\zeta_{l'})^3$		−0.75	−0.25	−1.5	−0.75

and where the variance $[\sigma(\mathrm{Sl})]^2$ can be computed exactly by means of Table IV of I and of *ab initio* values of the physical radial integrals.

(ii) The spin-orbit-dependent part μ_3^c(SOD) (the bottom line of Table I) computed exactly, using Table IV, which contains the numerical values of the coefficients written formally in Table II.

Two examples of application of this procedure are given in Table V, for Xe XXIX $3d^8$-$3d^7 4f$ and Pr XVI $4d^8$-$4d^7 4f$, and are compared with the exact values of μ_3^c computed by means of the explicit diagonalization of H in both configurations. To provide some detailed information, the exact values have been split in five parts, evaluated either from the formulas in Table II or from *ad hoc* diagonalizations. The relativistic-central-field code[8] (RELAC) and nonrelativistic approximation formulas[9] have yielded the *ab initio* values of the radial integrals used in the diagonalizations and in the calculation of σ(Sl).

In both cases the fair agreement, sufficient for our purpose, between the *exact* value of μ_3^c and its *hydrogenic-ratio* approximation supports the use of the latter. The two cases are quite different: in the Xe case the predominant contribution comes from the *BCC* term, and in the Pr case from the *BBB* term.

IV. REPRESENTATION OF SKEWED ARRAYS

A. The skewed Gaussian

The dimensionless constant which characterizes the skewness of a distribution is its asymmetry coefficient,

$$\alpha_3=\mu_3^c/(\mu_2^c)^{3/2}\ . \tag{7}$$

For representing an asymmetrical transition array by a continuous curve, we have chosen the skewed Gaussian shape proposed by Croxton *et al.*[10] and used by Cowan.[5] The corresponding function reads, within an arbitrary multiplicative factor,

$$f(x)=[1-\tfrac{1}{2}\alpha_3(x-\tfrac{1}{3}x^3)]e^{-x^2/2}\ , \tag{8}$$

where x is the reduced abscissa, measured in units of $\sigma=(\mu_2^c)^{1/2}$ (the rms deviation of the distribution), and referred to the reduced first moment μ_1/σ of the distribution.

If $\alpha_3\neq 0$, this function is not positive for all the values of x. But, for moderate values of α_3, the curve does not reach points far under the x axis, so that this negative part can be truncated in the drawing of a calculated spectrum. The examples of $\alpha_3=-1.0$ and -2.0 are shown in Fig. 2.

Now, the most interesting features of a broad peak observed in a spectrum are the wave number ν_m of its maximum and its FWHM $\Delta\nu$. For a Gaussian-shaped peak, $\nu_m\equiv\mu_1$ and $\Delta\nu=2(2\ln 2)^{1/2}\sigma=2.355\sigma$. But this is not true for the skewed-Gaussian distribution written in Eq. (8), for which we write, instead,

$$\nu_m=\mu_1+\delta\nu \tag{9}$$

and

$$\Delta\nu=2(2\ln 2)^{1/2}\sigma'\ . \tag{10}$$

TABLE V. Comparison of the contributions of the different types of parameter products to μ_3^c (in 10^{12} cm^{-3}) in Xe XXIX $3d^8$-$3d^7 4f$ and Pr XVI $4d^8$-$4d^7 4f$. $A=F^k(l,l)$, $B=F^k(l,l')$ and $G^k(l,l')$, $C=\zeta_l$ and $\zeta_{l'}$. Each entry with superscript a or b represents the sum of the terms of specified type.

	Explicit calculation						Hydrogenic approximation		
	AAA[a]	BBB[b]	CCC[a]	ABB and BAA[b]	BCC[a]	total μ_3^c	μ_3^c(Sl)	μ_3^c (SOD)	total μ_3^c
Xe XXIX $3d^8$-$3d^7 4f$	201.9	−193.4	55.9	−233.8	−475.1	−644.5	−245.5	−419.3	−664.8
Pr XVI $4d^8$-$4d^7 4f$	13.1	−332.0	1.0	196.4	−42.5	−163.9	−150.3	−41.5	−191.8

[a]Values obtained using the formulas presented in Table II.

[b]Values deduced from *ad hoc* diagonalizations and explicit calculations of μ_3^c.

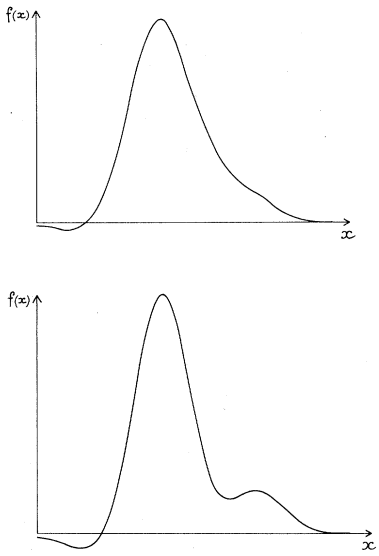

FIG. 2. The skewed Gaussian. The equation of this curve is $f(x)=c[1-\frac{1}{2}\alpha_3(x-\frac{1}{3}x^3)]e^{-x^2/2}$, α_3 is the asymmetry coefficient [Eq. (7)]. c is an arbitrary constant. In the upper curve, $\alpha_3=-1$; in the lower, $\alpha_3=-2$.

The quantities $\delta\nu/\sigma$ and σ'/σ are functions of α_3 only, which are drawn in Figs. 3 and 4. They are, respectively, an odd and an even function of α_3. The latter is a positive function not larger than 1; this means that an UTA with a given variance μ_2^c has a smaller FWHM if it is skewed than if it is symmetrical (up to about one-third, according to Fig. 4).

B. The example of Pr XVI $4d^8$-$4d^7 4f$

It is now possible to describe Fig. 1 completely.

(i) The dashed curve (a) is the *envelope* of the line array, in the sense that its ordinate is the superposition of 721 Gaussian curves, one per line, having each the relevant axis and height and a small FWHM (0.5 Å).

(ii) The symmetrical solid curve (b) is a Gaussian curve centered at $\nu=\mu_1$ and whose FWHM is equal to 2.355σ; it is the only possible description if only the first two moments of the distribution are available.

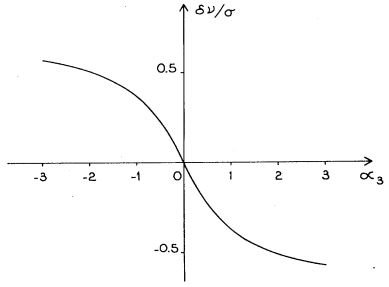

FIG. 3. Curve giving the ratio of the shift $\delta\nu$ of the maximum to the rms deviation σ, vs α_3, the coefficient of asymmetry.

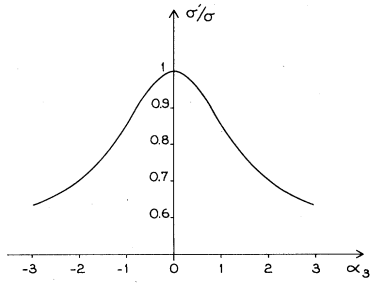

FIG. 4. Curve giving the ratio σ'/σ of the FWHM of the skewed Gaussian to that of the Gaussian, vs α_3, the coefficient of asymmetry.

(iii) The asymmetrical solid curve (c) is a skewed Gaussian [Eq. (8)], which peaks at $\nu=\nu_m$ (but remains centered at $\nu=\mu_1$), and with a FWHM equal to $2.355\sigma'$ [Eq. (10)]. Both ν_m and σ' are derived from *ab initio* radial integrals already used in Table V, yielding the asymmetry coefficient $\alpha_3=\mu_3^c/(\mu_2^c)^{3/2}=-1.79$. The negative part of this curve, on the short-wavelength side, has been deleted.

The maximum heights of the skewed Gaussian (c) and of the symmetrical curve (b) have been adjusted so that the areas under these curves are identical. The maximum height of the envelope (a) has been adjusted to be the same as that of the skewed Gaussian (c).

The fair agreement between curves (a) and (c), in position and width, and their disagreement with the symmetrical curve (b) support the validity of the skewed Gaussian description. However, the shoulder of the asymmetrical solid curve is an artifact of the skewed Gaussian function (see Fig. 2), and its resemblance to the shoulder of the envelope is fortuitous.

V. CONCLUSION

In conclusion, the present paper contains formulas and numerical tables which are sufficient for an easy evaluation of the asymmetry coefficient α_3 of the weighted wave-number distribution of the nl^{N+1}-$nl^N n'l'$ transition array. Thus, it is meaningful to describe this array in a

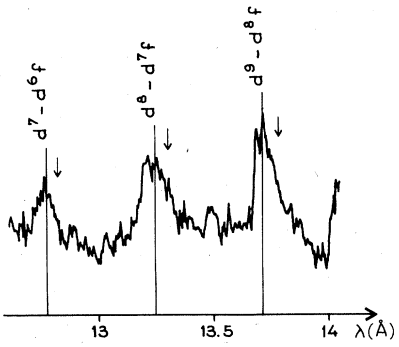

FIG. 5. Recording of the ionized Xe spectrum emitted by the TFR 600 tokamak (preliminary results). Xe XXVIII: $3d^9$-$3d^8 4f$. Xe XXIX: $3d^8$-$3d^7 4f$. Xe XXX: $3d^7$-$3d^6 4f$. The arrows indicate the position of the maximums calculated without taking into account the asymmetries of the patterns. The axes which are drawn are shifted by the quantity $\delta\nu$ (Sec. IV).

calculated spectrum by means of an asymmetrical skewed Gaussian curve. The axis and FWHM of this curve are quite different from those of the simple Gaussian curve proposed previously: in brief, asymmetry results in a shift of the maximum and a narrowing of the peak. Once the values of σ and α_3 are known, the shift and the FWHM can be readily derived from Figs. 3 and 4. The steep slope of the curve is on its long- (short-) wavelength side if α_3 is positive (negative).

In Table V we present the detailed numerical contributions to the third-order moment for two different physical arrays, one where the largest contribution comes from the Slater integrals (Pr) and one where it comes from the spin-orbit integrals (Xe). If the spin-orbit integrals were still larger, one would, of course, observe a spin-orbit-split array,[11] for which the asymmetry coefficient of the total array is meaningless.

Experimental examples can be seen in a spectrum recently obtained on the TFR 600 tokamak at Fontenay-aux-Roses on a preliminary recording with low resolution. They consist of three transition arrays of Xe XXVIII—XXX, namely $3d^9$-$3d^8 4f$, $3d^8$-$3d^7 4f$, and $3d^7$—$3d^6 4f$, shown in Fig. 5. All three features have their steep slope on the short-wavelength side, corresponding to negative values of α_3, e.g., -1.55 for $3d^8$-$3d^7 4f$ (see the value of μ_3^ζ in Table V). For each array, the arrow indicates the place where the maximum of the Gaussian curve would be if the asymmetry was overlooked.

ACKNOWLEDGMENT

We thank the TFR group at Fontenay-aux-Roses for communicating to us the preliminary recording of a Xe spectrum.

[1]C. Bauche-Arnoult, J. Bauche, and M. Klapisch, Phys. Rev. A **20**, 2424 (1979).

[2]C. Bauche-Arnoult, J. Bauche, and M. Klapisch, J. Opt. Soc. Am. **68**, 1136 (1978); Phys. Rev. A **25**, 2641 (1982).

[3]M. Klapisch, E. Meroz, P. Mandelbaum, A. Zigler, C. Bauche-Arnoult, and J. Bauche, Phys. Rev. A **25**, 2391 (1982); M. Klapisch, J. Bauche, and C. Bauche-Arnoult, Phys. Scr. T3, 222 (1983).

[4]S. A. Moszkowski, Prog. Theor. Phys. **28**, 1 (1962).

[5]R. D. Cowan, *The Theory of Atomic Structure and Spectra* (University of California, Berkeley, 1981), Chap. 21.

[6]B. R. Judd, *Second Quantization and Atomic Spectroscopy* (Johns Hopkins University, Baltimore, 1967).

[7]B. R. Judd, *Operator Techniques in Atomic Spectroscopy* (McGraw-Hill, New York, 1963).

[8]E. Luc-Koenig, Physica (Utrecht) **62**, 393 (1972); M. Klapisch, J.-L. Schwob, B. S. Fraenkel, and J. Oreg, J. Opt. Soc. Am. **67**, 148 (1977).

[9]F. P. Larkins, J. Phys. B **9**, 37 (1976); J. Bauche, C. Bauche-Arnoult, E. Luc-Koenig, and M. Klapisch, *ibid.* **15**, 2325 (1982).

[10]F. E. Croxton, D. I. Cowden, and S. Klein, *Applied General Statistics,* 3rd. ed. (Prentice-Hall, Englewood Cliffs, 1967), Chap. 10, p. 533.

[11]C. Bauche-Arnoult, J. Bauche, and M. Klapisch (unpublished)